AIAS 2019 International Conference on Stress Analysis

Modelling and Experimental Testing of Thick CFRP Composites Subjected to Low Velocity Impacts

Alvaro Gonzalez-Jimenez[a]*, Andrea Manes[a], Alessio Beligni[a], Michał Dziendzikowski[b], Claudio Sbarufatti[a], Marco Giglio[a]

[a]Politecnico di Milano, Dipartimento di Meccanica, via La Masa 1, Milano 20155, Italy
[b]Air Force Institute of Technology, ul. Ks, Boleslawa 6, 01-494 Warszawa, Poland

Abstract

The present paper investigates a modelling approach of experimentally tested thick panels made of Carbon Fibre Reinforced Polymers (CFRP). The coupons were made of 24 unidirectional (UD) laminae with a layup $[45/0/-45/90]_{3s}$. The specimens were subjected to low velocity impact using a drop tower system. Several sensors, including a load cell and strain gauge, were utilized both for analysing the behaviour of the material against the impact and for performing a validation of the numerical models. Three energy levels were adopted: 8J, 10J and 12J.

Numerical models were implemented into the finite element (FE) software LS-DYNA. A linear - elastic constitutive law with an instantaneous failure material was selected for mimicking the intralaminar behaviour of the carbon fibre composite. Enhanced Chang – Chang was adopted as the onset-of-failure criterion. This criterion is able to capture damage in different directions and permits the consideration (or not) of the shear behaviour in the failure equations. The capability of the model to capture the correct interface failure process was particularly emphasized and therefore cohesive elements with a bilinear traction – separation law were chosen for the reproduction of delamination. Finally, the experimental – numerical results were compared using first and foremost the overall delamination area and the curves force – time, force – displacement and absorbed energy – time as well as the strain measures obtained by the sensors.

* Corresponding author. Tel.: +39 02.2399.8668; fax: +39-02 2399 8263.
E-mail address: alvaro.gonzalez@polimi.it

1. Introduction

Composites materials have become one of the most efficient choices in the design of mechanical structures since they provide a high strength/stiffness to weight ratio. However, they are also vulnerable to out-of-plane low energy impact loads which might generate damage that could significantly decrease the load bearing properties of the structure remaining hidden to the naked eye. This is usually referred to as barely visible impact damage. This fact is combined with the complex failure process of composites which might involve failure mechanism such us fibre breakage, fibre – matrix debonding, matrix cracking or delamination. It is therefore important to be able to predict the failure behaviour of composite materials and, among the potential methodologies, numerical simulations provide a cost efficient and relatively fast solution.

In the analysis of all impact events, the study of low velocity impacts is potentially useful since composites are increasingly used in aeronautic structures that might be subjected to impact by debris, birds or even dropped tools during the manufacturing process or maintenance. Focusing on the damage prediction capability, numerical approaches are preferred due to their potential to consider the complex failure processes. Among the available software LS-DYNA is widely used in the literature for simulating low velocity impact events. It provides a wide library of composite material models and of contact algorithms, including cohesive material models. Particularly, material model number 54 (MAT54) provides a good precision – to parameter - requirement ratio. Heimbs *et al* (Heimbs, Heller, Middendorf, Hähnel, & Weiße, 2009) used MAT54 for simulating a low velocity impact event on Carbon Fibre Reinforced Polymers (CFRP) with preloading. They obtained very accurate results in terms of force – time and energy – time curves although due to the typology of the model used (*i.e.* less interfaces than the real model) they failed to reproduce the delamination obtained experimentally. There are several failure criteria which have proven to correctly mimic impact events. Liu *et al* (Liao & Liu, 2017) utilized a user – defined material subroutine (VUMAT) in the software ABAQUS for testing several material models for the specific case of a low velocity impact on unidirectional CFRP. They reached the main conclusions that the Puck criteria (Puck & Schürmann, 2004) was the most adequate. This criteria, different from Chang – Chang (Chang & Chang, 1987) or Hashin (Hashin, 1980) considers an sloped fracture plane for the matrix compression. However, this material models requires very specific experimental parameters which are cumbersome to obtain.

Additionally, to the intralaminar behaviour of the material, the consideration of the interlaminar response of the composite material is also important. Long *et al* (Long, Yao, & Zhang, 2015) performed a simulation of a low velocity impact on CFRP using the Hashin intralaminar failure model and cohesive elements with a bilinear traction – separation law for the simulation of the failure due to delamination. They obtained good experimental – numerical agreement reaching the conclusion that the delamination propagates larger in the interfaces opposite the impact layer and always in the direction of the fibres of the lower ply for each interface considered. It is widely believed that matrix cracking failure is directly coupled to the creation of delamination (Borg, Nilsson, & Simonsson, 2004) and might guide the directionality of the delamination process (Sun, Kawashita, Kaddour, Hiley, & Hallett, 2018). Previously, authors have proposed models accounting for this fact (Hongkarnjanakul, Bouvet, & Rivallant, 2013) however these models potentially makes the acquisition of results cumbersome and requires a large quantity of input parameters.

In the present study, the numerical simulation of several low velocity impacts tests on angle-ply carbon fibre/epoxy composites at different energies (i.e. 8J, 10J and 12J) was implemented using the software LS-DYNA. The intralaminar behaviour was mimicked using the Chang – Chang failure onset criteria while the interlaminar damage process was modelled using cohesive interfaces with the possibility of simulating Mode I, Mode II and mixed mode using a power law. The results are presented in terms of force, energy, displacement, strain and delamination.

2. Experimental set-up and specimen configuration

Low velocity impacts were performed through a drop - tower methodology according to standard ASTM D7136((ASTM), 2015). Three level of energies were employed: 8J, 10J and 12J. The impactor tip has a hemispherical shape of 16 mm diameter with a total weight of 1.325 kg.

During the impact events, the evolution of the contact force was recorded using a load cell which was positioned between the impactor tip and the group of masses added. As and additional activity, the evolution of strain

in certain points was measured using biaxial strain gauges and a Fibre Bragg Grating (FBG) sensor.

The position of the strain sensors utilized is shown in Figure 1. The schematised steel frames which held the specimen is represented in yellow, while the specimen itself is represented in black.
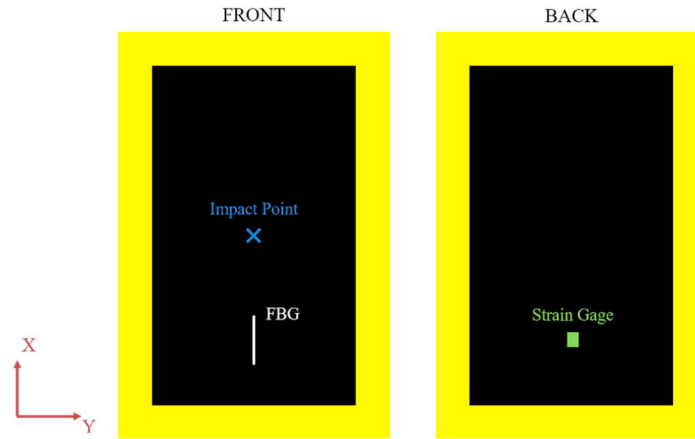

Figure 1 Position of the sensors

The material used is composed of unidirectional pre-preg laminae CYCOM® 977-2-34%-24K IMS-196-T1 made of carbon fibres embedded into epoxy resin. The laminate is formed of 24 layers with a layup of [45°, 0°, -45°, 90°]$_{3s}$. The 150 x100 mm size of the specimens was selected as specified in the standard ((ASTM), 2015) with a thickness of 4.8mm which results in a layer thickness of 0.2 mm. The mechanical properties of the material were experimentally obtained. All the parameters are presented in Table 1.

Table 1 Mechanical parameters for the material used

Variable	Acronym	Value	Source
Density	ρ	1.62 [g/cm^3]	Rule of mixture
Modulus of elasticity in direction 1	E_1	157.49 [MPa]	Experimental
Modulus of elasticity in direction 2	E_2	9.95 [MPa]	Experimental
Shear modulus in direction 12	G_{12}	4.95 [MPa]	Experimental
Poisson ratio in direction 12	ν_{12}	0.24 [-]	Experimental
Tensile strength in direction 1	X_t	2550 [MPa]	Experimental
Tensile strength in direction 2	Y_t	57.4 [MPa]	Experimental
Compressive strength in direction 1	X_c	1365 [MPa]	Experimental
Compressive strength in direction 2	Y_c	202 [MPa]	Experimental
Shear strength in direction 23	S_{23}	89 [MPa]	Experimental

The modulus of elasticity in direction 3 (E_3) was considered equal to E_2. The shear modulus in direction 13 was also considered equal to G_{12} while the shear modulus in direction 23 was calculated using E_2 and ν_{23}. The Poisson coefficient in direction 23 (ν_{23}) was taken from the literature (Yun, An, Gao, & Yue, 2017) while ν_{13} was considered as ν_{12}. The density was computed through the rule of mixture.

3. Numerical modelling

In order to reduce computational time, some simplifications were assumed in the numerical model with

respect to the real experimental set-up. First, only one quarter of the model was implemented (*i.e.* in-plane dimensions of 75 x 50 mm) and the pertinent symmetry conditions were applied. Second, the real experimental fixture of the specimen was not implemented instead, all the nodes which belong to the border of the part of the specimen outside the metallic fixture, in yellow in Figure 1, were fixed (*i.e.* all degrees of freedom were blocked).

Due to the considerable thickness of the specimen the correct consideration of the out-of-plane load transmission is of utmost importance and hence linear solid elements made of 8 nodes and with a reduced integration (*i.e.* one integration point for each element) were used for modelling the layers of the composite. In order to improve the computational time efficiency, only one element was built along the thickness of each layer. Consequently, the considered dimension of the intralaminar elements were 1 x 1 x 0.2 mm.

Due to the high stiffness of the impactor in comparison with the composite, it was assumed to be rigid without committing a significant error. The impactor was modelled with linear 8-node brick elements with reduced integration and the initial velocity was equal to the one experimentally measured.

In layered materials, delamination potentially represents a great amount of energy dissipation (Heimbs *et al.*, 2009) and consequently, it might result a cause of failure. Furthermore, delamination results more critical in low velocity impact cases since it might remain hidden to the naked eye, but which could cause a significant decrease in the load – bearing capability of the structure. Therefore, the accurate prediction of delamination using predictive methods such as numerical simulation is of great importance. In the present study cohesive elements were used for modelling the interface of the CFRP. One cohesive layer for each interface was implemented for a total of 23. The out-of-plane dimensions of the cohesive layers should be small enough not to influence the elastic properties of the whole composite. Considering this condition, cohesive elements of 1 x 1 x 0.001 mm dimension were selected, and the element formulation selected was solid cohesive elements with 8 nodes and 4 integration points.
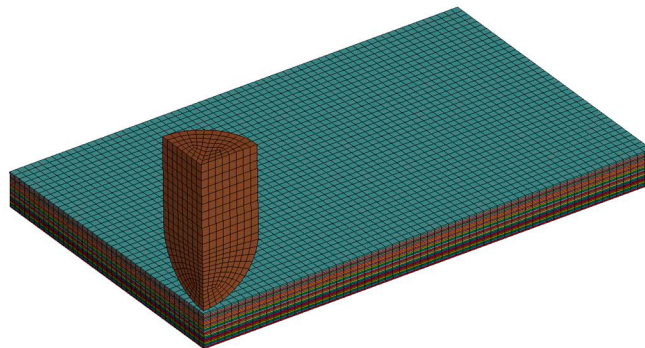

Figure 2 Numerical model representation

With regards to the material models, the Chang – Chang failure onset criteria (Chang & Chang, 1987) with a post-damage behaviour defined by a residual strength parameter (i.e. SLIM*X*) was utilized. This post damage behaviour was activated only for compressive load in direction 2 (i.e. matrix direction) and for shear. For the case of tensile and compressive loads in direction 1 (*i.e.* fibre direction) and tensile loads in direction 2 the material behaves as an instantaneous failure material in which the stiffness of the elements is reduced to zero when the limit strength defined by Chang – Chang criterion is met. It is worth clarifying that even if one element reaches the failure onset, it will not be eliminated from the simulation until a user – defined cancellation criteria is met. For the present case, the cancellation criteria followed is based on the time step: the user must define a time step below which the element will be removed or, in other words, when the element reaches a limit distortion, it will be cancelled. This parameter is numerical and should be defined through an iterative process for each study case. For the actual work, the time step was set to 0.93. For further references, the LS-DYNA manual Volume II (Livermore Software Technology Corporation (LSTC), 2017).

A bilinear traction – separation law with the possibility of considering Mode I, Mode II and their interaction (*i.e.* mixed mode capability) through a power law was used for the cohesive material, specifically, the cohesive material number 138 of LS-DYNA. In this case, two out of three possible parameters for each Mode have to be

defined. The possible parameter to be defined are interface limit strength, critical energy release rate or limit of separation among the two cohesive faces. In the present analysis, the input parameters were the critical energy release rate in Mode I (i.e. G_{Ic}) which was equal to 0.545 J/m^2, critical energy release rate in Mode II (i.e. G_{IIc}) which was equal to 1.387 J/m^2 and the strength of the interface in tension (*i.e.* Mode I) which was equal to 81.4 MPa and in shear (i.e. Mode II) which was equal to 97.6 MPa. These parameters were obtained from (Ilyas, Lachaud, Espinosa, & Salaün, 2009) for a similar material. Figure 2 shows an image of the final model.

4. Results and discussion

In this section, the experimentally obtained results are subdivided into three subsections *i.e.* the load cell, delamination and strain sensors. Each of them is presented together with the numerically obtained data.

1.1. Load cell results

The experimental results as well as the experimental – numerical comparison were analysed in three curves: force – time, force – displacement and energy – time curve. The data vector of displacement and energy were computed from the force data (acquired by the load cell) as specified in the standard ((ASTM), 2015). Also, the experimentally obtained data were filtered using a low pass filter set at 6kHz. This limit frequency was set as suggested in the standard ((ASTM), 2015) which distinguishes between oscillations created by the natural frequencies of the impactor (*i.e.* impactor ringing) and the oscillations created by the flexural vibration of the specimen. The former oscillations have a larger frequency than the latter and therefore can be filtered without the loss of meaningful information. The results for the force – time, force – displacement and energy – time curves for all impact energies are shown in Figure 3.

Good agreement in terms of maximum force reached (see Figure 3a1-b1-c1) as well as in terms of total energy absorbed (*i.e.* a plateau – like trend in Figure 3a3-b3-c3) is clearly visible. The oscillations observed on the experimental curves and not on the numerical ones are, most certainly, due to unrealistic viscous damping present on the numerical model (Lopes, Sádaba, González, Llorca, & Camanho, 2016). Even if good agreement in overall terms was reached, the numerical model was unable to correctly reproduce the damage initiation phenomenon (*i.e.* the first force drop on the force – time curves). This inaccuracy is most likely due to the fact that the material model 54 does not correctly considered the existence of a rotated fracture plane on composites due to matrix compression (Liao & Liu, 2017). Apart from this inaccuracy, the numerical model overpredicts the flexural stiffness of the experimental specimens (*i.e.* the slope of a straight line fitted on the force – displacements curves from the origin to the point of maximum force) and slightly underpredict the maximum displacement. Probably caused by the choice of the fixing constrain that does not reproduce the possible slipping of the panels inside the gripping fixture.

1.2. Delamination results

For the prediction of interlaminar failure by the numerical model, once a cohesive element was removed from the simulation it was regarded as failed. The delaminated area was then measured as the outer profile of the removed elements.

In the experimental tests, the outer profile of the delamination was measured using a non -destructive ultrasonic method. The numerical – experimental comparison of the outer profiles is presented in Figure 4. clearly showing that the outer profile was well mimicked with error percentages of 6.2%, 1% and 2.6% for the energies of 8J, 10J and 12J respectively. The error in the delamination profile is most likely caused by the fact that only one quarter of the whole specimen was considered for the numerical model. However, the lack of delamination prediction precision is widely overcome by the simulation efficiency gained.
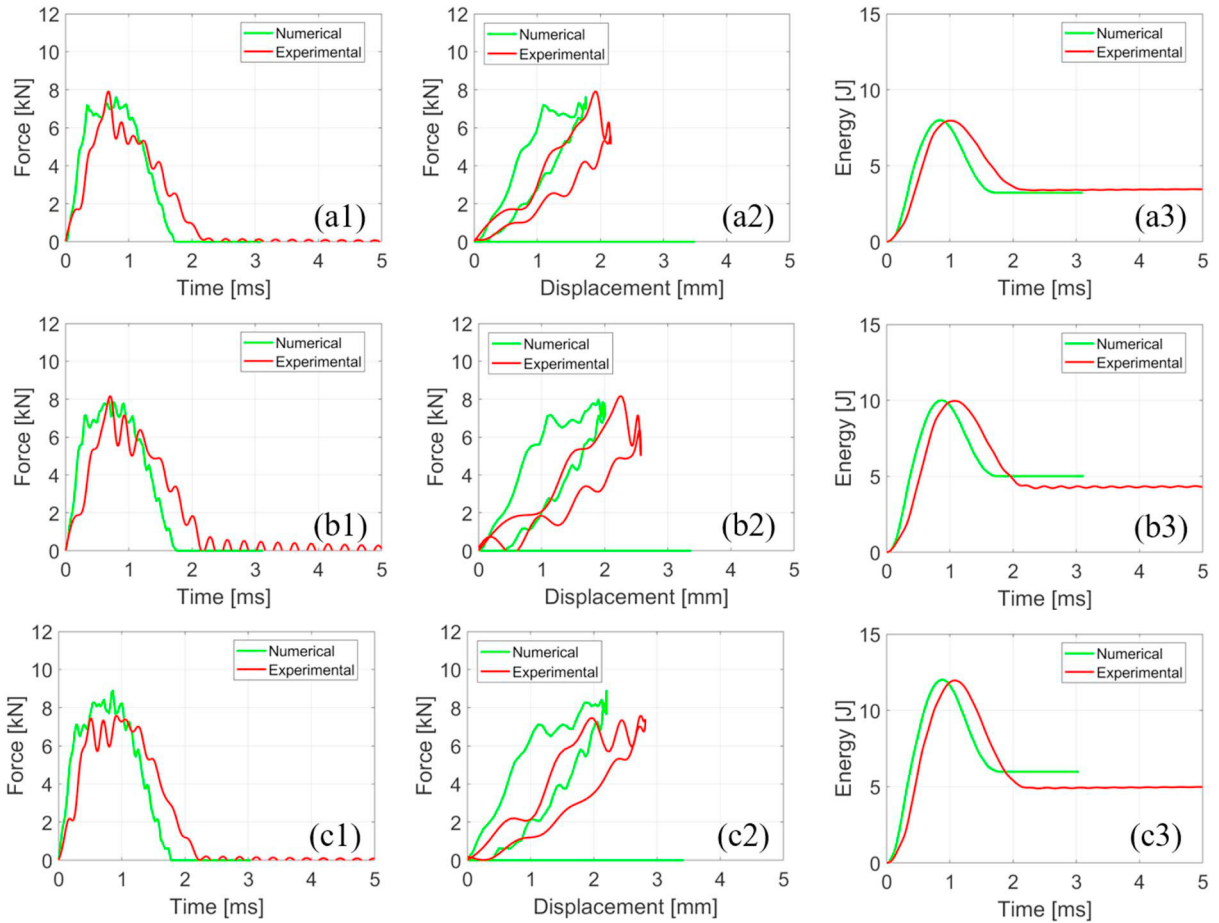
Figure 3 Comparison of numerical and experimental load cell results: (a) 8J, (b) 10J and (c) 12J.

1.3. Strain sensors results

As aforementioned, during the experimental impact events, two type of sensors were placed which acquired the strain evolution over time. One sensor was a biaxial strain gauge (global directions X and Y in Figure 1) placed on the back layer of the specimen (*i.e.* the layer opposite the impact) and the other sensor was a FBG sensor positioned on the layer impacted (longitudinal or X direction). For the numerical case, a specific procedure to obtain strain measurements as similar as possible to the experimental one was set up. Therefore, initially the length and the position of the actual sensor was measured and the nodes of the model which, virtually, lie underneath the sensor were considered; subsequently, in the numerical simulation, the change of length among two consecutive nodes in the direction of interest was measured. This change of length was divided by the undeformed element length and the resultant number was regarded as the strain of the specific element considered. This was performed for each couple of nodes lying underneath the sensor and an average was done. Finally, the value for each step (*i.e.* time) considered in the simulation was plotted forming the strain – time evolution curve.

The numerical – experimental comparison is shown in Figure 5. Observing the signals for the strain gauge in the longitudinal direction (see Figure 5a), the minimum value observed was relatively good capture by the numerical model. In the case of the strain gauge in the transversal direction (Figure 5b), the opposite happened: the trend of the experimental signals was captures relatively well but the numerical model underpredicted the maximum strain. For the case of the experimental signal of the FBG (red curves in Figure 5c) a saturation of the fibre signal happened at ±

200 με which generated a cut off in the experimental signal. It is worth to mention that the optical interrogator used for the FBG strain acquisition has been specifically designed and built for an alternative activity, that has the aim of capturing phenomena for which the ± 200 με limits are considered adequate. Obviously, this limitation is not present in the virtual sensor that replicates the fibre signal in the model and a complete simulated trend of the signal is present.

It must be considered that the numerical model implemented does not account for the fibre and the matrix as separate entities or, in other terms, a macro – homogeneous model and not a meso – heterogeneous one was employed in the present work. This fact might prevent the model from precisely predicting the strain wave propagated during the impact event leading to partially imprecise results. The procedure of building a meso – heterogeneous model is complex and time-consuming, and the computational time required for these kinds of models is high. Consequently, the prediction of the strain in macro – homogeneous models should be regarded as a qualitative activity rather than an accurate prediction of the strain level at particular points. Moreover, the sensors can acquire higher dynamics in the strain signals if compared to the strain time histories obtained by the simulation. This is due to the fact that the sensors are acquired at a frequency of 50 kHz and 100 kHz for the strain gauge and FBG, respectively; conversely, the numerical simulation is able to give a signal that is sampled at a frequency of 10kHz, as simulation efficiency and computational efforts are of major concern. Again, the motivation of having different acquisition frequencies is related to the fact that an alternative activity has been executed acquiring the strain signals, as already aforementioned.
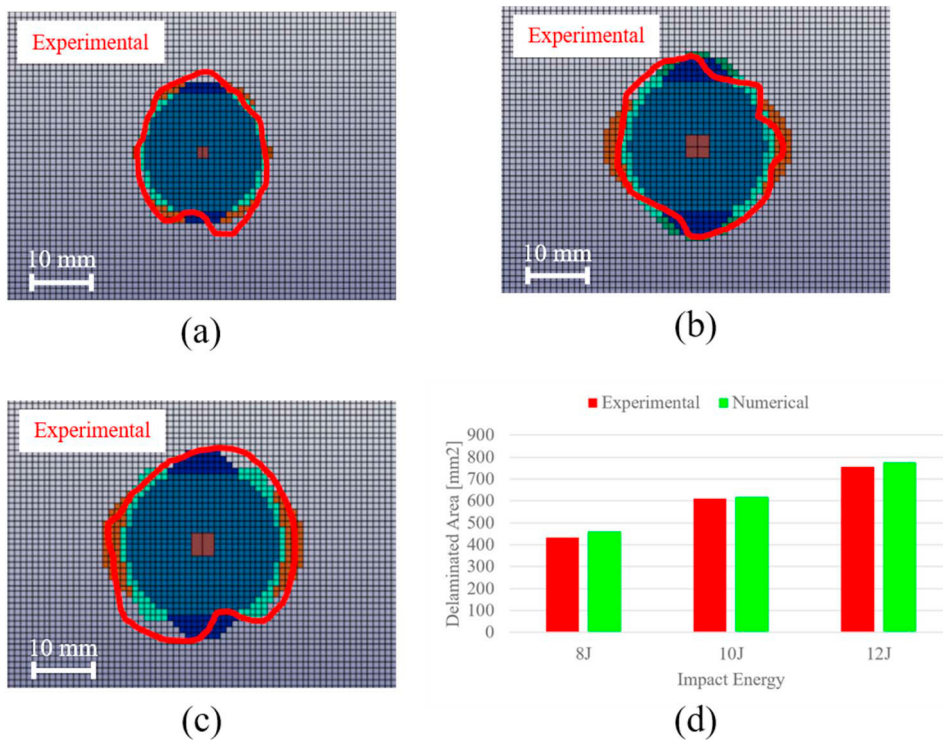

Figure 4 Comparison between numerical and experimental delamination for impact energies of (a) 8J, (b) 10J, (c) 12J; (d) comparison between numerical (green) and experimental (red) measured delaminated areas
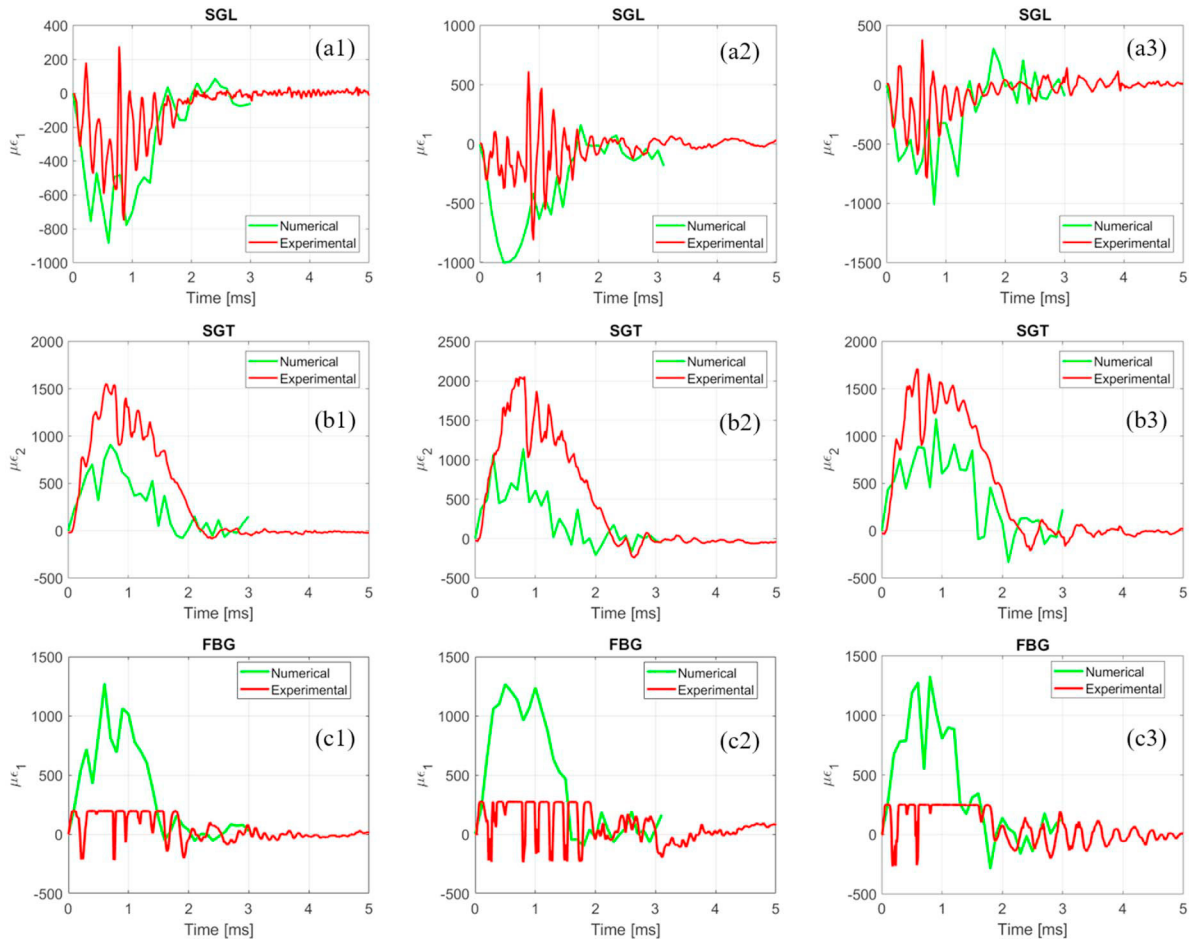
Figure 5 Comparison of numerical and experimental results for the strain gauge in the longitudinal direction (a), the strain gauge in the transversal direction (b) and the FBG (c) for the impact energies of 8J (1), 10J (2) and 12J (3)

5. Conclusions

In the present work, a numerical model of a low velocity impact on an angle-ply carbon fibre/epoxy was implemented in LS-DYNA for three impact energy levels. The intralaminar behaviour was simulated using the available MAT54 which is based on the Chang – Chang failure onset criterion. The interlaminar failure process was simulated employing a cohesive zone method approach using a bilinear traction – separation law while also considering mixed modes scenarios.

Very good agreement between numerical and experimental results was reached for the delamination prediction as well as good agreement in terms of predicted maximum contact force and total energy absorbed by the composite during the impact event. The numerical model was not fully able to capture quantitatively the values of strain reached in the experiment although reasonable prediction was achieved; however, the latter is left as future research by the authors. Finally, it is worth to mention that present work is also of interest for Structural Health monitoring approaches, thus able to use the results of such simulations in order to train algorithms for impact and damage assessment, Corbetta *et al.* (2014), Corbetta *et al.* (2015), Sbarufatti *et al.* (2017).

References

ASTM, A. S. of T. M. (2015). Standard Test Method for Measuring the Damage Resistance of a Fiber-Reinforced Polymer Matrix Composite to a Drop-Weight Impact Event. *ASTM International. Designation: D, i*(C), 1–16. https://doi.org/10.1520/D7136

Borg, R., Nilsson, L., & Simonsson, K. (2004). Simulation of low velocity impact on fiber laminates using a cohesive zone based delamination model. *Composites Science and Technology*, *64*(2), 279–288. https://doi.org/10.1016/S0266-3538(03)00256-2

Chang, F., & Chang, K.-Y. (1987). A Progressive Damage Model for Laminated Composites Containing Stress Concentrations. *Composite Materials*, 21(September), 834–855.

Corbetta, M., Sbarufatti, C., Manes, A., Giglio, M. On Dynamic State-Space models for fatigue-induced structural degradation (2014) International Journal of Fatigue, 61, pp. 202-219.

Corbetta, M., Sbarufatti, C., Manes, A., Giglio, M. Real-time prognosis of crack growth evolution using sequential Monte Carlo methods and statistical model parameters (2015) IEEE Transactions on Reliability, 64 (2), art. no. 6953312, pp. 736-753.

Hashin, Z. (1980). Failure Criteria for Unidirectional Fiber Composites. *Journal of Applied Mechanics*, *47*(2), 329. https://doi.org/10.1115/1.3153664

Heimbs, S., Heller, S., Middendorf, P., Hähnel, F., & Weiße, J. (2009). Low velocity impact on CFRP plates with compressive preload: Test and modelling. *International Journal of Impact Engineering*, *36*(10–11), 1182–1193. https://doi.org/10.1016/j.ijimpeng.2009.04.006

Hongkarnjanakul, N., Bouvet, C., & Rivallant, S. (2013). Validation of low velocity impact modelling on different stacking sequences of CFRP laminates and influence of fibre failure. *Composite Structures*, *106*, 549–559. https://doi.org/10.1016/j.compstruct.2013.07.008

Ilyas, M., Lachaud, F., Espinosa, C., & Salaün, M. (2009). Dynamic delamination of aeronautic structural composites by using cohesive finite elements. *17th International Conference on Composite Materials (ICCM-17)*, 27–31.

Liao, B. B., & Liu, P. F. (2017). Finite element analysis of dynamic progressive failure of plastic composite laminates under low velocity impact. *Composite Structures*, *159*, 567–578. https://doi.org/10.1016/j.compstruct.2016.09.099

Livermore Software Technology Corporation (LSTC). (2017). LS-DYNA: Keyword User Manual Volume 2.

Long, S., Yao, X., & Zhang, X. (2015). Delamination prediction in composite laminates under low-velocity impact. Composite Structures, 132, 290–298. https://doi.org/10.1016/j.compstruct.2015.05.037

Lopes, C. S., Sádaba, S., González, C., Llorca, J., & Camanho, P. P. (2016). Physically-sound simulation of low-velocity impact on fiber reinforced laminates. International Journal of Impact Engineering, 92, 3–17. https://doi.org/10.1016/j.ijimpeng.2015.05.014

Puck, A., & Schürmann, H. (2004). Failure analysis of FRP laminates by means of physically based phenomenological models. Failure Criteria in Fibre-Reinforced-Polymer Composites, 3538(96), 832–876. https://doi.org/10.1016/B978-008044475-8/50028-7

Sbarufatti, C., Beligni, A., Gilioli, A., Ferrario, M., Mattarei, M., Martinelli, M., Giglio, M., Strain wave acquisition by a fiber optic coherent sensor for impact monitoring (2017) Materials, 10 (7), art. no. 794.

Sun, X. C., Kawashita, L. F., Kaddour, A. S., Hiley, M. J., & Hallett, S. R. (2018). Comparison of low velocity impact modelling techniques for thermoplastic and thermoset polymer composites. Composite Structures, 203(March), 659–671. https://doi.org/10.1016/j.compstruct.2018.07.054

Yun, Y., An, L., Gao, G., & Yue, X. (2017). Effect of Liquid Shim on the Stiffness and Strength of the Composite-composite Single Lap Joint. DEStech Transactions on Materials Science and Engineering, (ammme), 4–9. https://doi.org/10.12783/dtmse/ammme2016/6901